COMMISSIONING OF THE BESSY II BOOSTER SYNCHROTRON

M. Abo-Bakr, W. Anders, R. Bakker, T. Birke, K. Bürkmann, V. Dürr, W. Gericke, M. v. Hartrott, E. Jaeschke, D. Krämer, B. Kuske, P. Kuske, M. Martin, R. Müller, K. Ott, J. Rahn, T. Schneegans, G. Wüstefeld and E. Weihreter, BESSY, Berlin, Germany

Abstract

The injection system for the 3rd generation synchrotron light source BESSY II became operational in April 1997. It consists of a 50 MeV microtron and a rapid cycling 1.9 GeV low emittance synchrotron, which ensures a short filling time. Commissioning results including beam optical measurements at injection energy and during acceleration are reported to characterize the performance and the main parameters of the synchrotron.

1 INTRODUCTION

The basic design goal for the BESSY II injection system was to provide a beam intensity large enough to fill the storage ring at full energy of 1.9 GeV in multibunch operation to 200 mA in typically one minute. Table 1 recalls the main parameters of the system. The details of the optics [1, 2], the layout of the magnets [3], and White circuits [4], and of the transfer lines [5] have been presented elsewhere. Here we concentrate on operational experience and beam optical measurements made during commissioning.

Table 1: Main Parameters for the BESSY II Synchrotron

Max. energy E_{max}	[GeV]	1.9
Circumference L	[m]	96.
Repetition rate	[Hz]	10.
Number of cells N		16
Inj. energy E_{inj}	[MeV]	50.
B-field @ E_{max}	[T]	0.95
Emittance ε @ E_{max}	[m · rad]	$1.9 \cdot 10^{-7}$
Tunes Q_x/Q_z		4.42/3.38
Mom. compaction α		0.054
Nat. chromaticities ξ_x/ξ_z		-4.7/-3.9
Current (multibunch) I_b	[mA]	3
Rf-frequency f_{rf}	[MHz]	499.66

2 DC-MODE OPERATION AT 50 MEV

To optimize the injection process and verify the linear optics before switching on the White circuits, we operated the synchrotron as a storage ring at injection energy. After proper adjustment of the injection transfer line up to 4.5 mA of beam current have been stored with 6 mA from the microtron, giving a total transfer efficiency of 75% (transparency of transfer line $\approx$ 88%, injection efficiency $\approx$85%) We attribute the high injection efficiency to the favorable beam characteristics of the microtron offering

low emittance ($\varepsilon \approx 5 \cdot 10^{-7}$ m·rad) and small energy spread ($\Delta E/E \approx 2 \cdot 10^{-3}$).

2.1 *Tunes and β–Functions*

The lattice is based on a FODO structure where the dipole in every second cell is missing and the straight section has been reduced to 2.3 m. The design tunes ($Q_{x/z}$ = 4.42/3.38) were chosen near a half integer to reduce the sensitivity of the orbit to field and alignment errors [1]. To optimize the beam intensity, the tunes have been varied over a large range as shown in Fig. 1. In reasonable distance from major resonances no pronounced tune dependence of the beam current was observed giving a large freedom in tune space. Measurements of the mean β-functions in the quads agree well with the model optics.
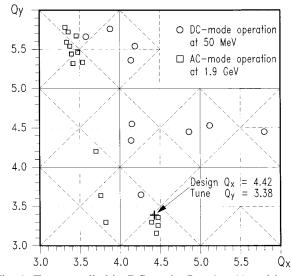

Fig. 1: Tunes studied in DC-mode (I $\geq$ 4 mA) and in the acceleration mode at full energy (I $\geq$ 2 mA).

2.2 *Orbit and Coupling*

For orbit correction 30 steerers are available with small DC power supplies allowing correction only at low energy. It turned out, however, that no steerers were needed to obtain the maximum beam current. Excitation of individual steerers indicates that the available free aperture around the real orbit is roughly $\Delta x \pm 15$ mm and $\Delta z \pm 6$ mm. Figure 2 shows the beam orbit measured with 30 BPM stations located near the quadrupoles, giving rather small maximum deviations of $\Delta x = \pm 4$ mm

and $\Delta z = \pm 2$ mm. BPM positioning errors are of the order of 1 mm in both planes. The vertical orbit errors, dominated by quadrupole displacements, are in reasonable agreement with the rms neighbour to neighbour alignment error of $\sigma_z = 0.15$ mm. Horizontally the orbit errors are caused mainly by deviations of the bending strength between the dipole magnets due to remanence effects.
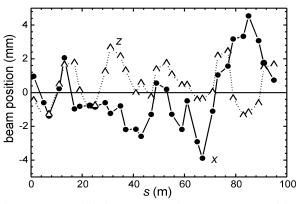

Fig. 2: Beam orbit in DC-operation at 50 MeV without excitation of steerer magnets.

A rather small coupling of $|k| = 8 \cdot 10^{-3}$ has been obtained from measurements of the stopband width by varying the tunes near the difference resonance $Q_x - Q_z = -2$. With the conservative assumption that the rms rotation of the quadrupoles around the beam axis is $\Theta_{rms} = \pm 0.2$ mrad, a coupling strength of only $|k| = 8 \cdot 10^{-4}$ is expected. A second contribution to the coupling can be attributed to a relatively strong sextupole term of the dipoles which was measured at low field for the prototype magnet ($m \cdot l = 0.7$ m^{-2}). Assuming a vertical rms orbit deviation of 2 mm in the dipoles gives a coupling of about $2 \cdot 10^{-3}$ which dominates the contribution from quadrupole tilts. Together with the orbit observations these findings indicate that the magnets are aligned sufficiently well.

3 BEAM ACCELERATION

3.1 Operation of White Circuits

Three White circuits operating at $f_{rep} = 10$ Hz are used to excite independently the dipoles, the focussing quads and the defocussing quads with a field function

$$B\,(t) = B_{DC} - B_{AC} \cdot \cos\,(2\,\pi\,f_{rep}\,t),$$

where the AC and DC fields are generated by independent power supplies. A relative tracking error between the families not larger than $2.6 \cdot 10^{-4}$ can be tolerated to limit the tune variation during acceleration to $\delta Q \leq \pm 0.05$ in both planes. The AC current of each circuit is generated by an IGBT (isolated gate bipolar transistor) H-bridge inverter, which provides a high purity 10 Hz sine wave current. Generation of odd harmonics (as in the case of a

rectangular voltage inverter) is therefore strongly suppressed. This has the advantage that only even harmonics from saturation effects in the magnets and chokes contribute to the tracking errors.

The three AC power supplies are driven by individual sine wave generators, where the dipole generator acts as a master and the quadrupole circuits are phase locked to the dipole circuit with the help of zero-cross signals. These signals are derived from sensing coils installed in the gaps of the reference magnets powered in series with the lattice magnets. As a result the phase of the quadrupole fields can be kept within ± 1 μs relative to the dipole field. The injection process is triggered by the signal from a peaking strip in the field of the reference dipole. To generate the desired guide field with minimum tracking error, the AC and DC currents of each circuit (i.e. six parameters) must be adjusted such that the amplitude ratio $\alpha = B_{DC}/B_{AC}$ is the same. This can be checked by peaking strips installed in the gap of the reference magnets, measuring the time difference Δt between the signal maxima given by

$$\Delta t = \frac{1}{2\pi f_{rep}}\,acos\big(B_{DC} \,/\, B_{AC}\big)$$

The remaining three parameters then define the energy and the tunes of the desired optics.

3.2 Tune and Chromaticity during Acceleration

Also in the AC-mode of operation different tunes have been studied demonstrating the large flexibility of the lattice. To measure the tune at different energies, the beam has been excited via striplines by a sinusoidal wave train of 200 μs length oscillating at the betatron frequency. The wave train was properly triggered by a variable delay to cover the whole acceleration cycle. With a digital scope operated in the FFT-mode the beam signal from a second stripline can then be analysed in frequency domain.
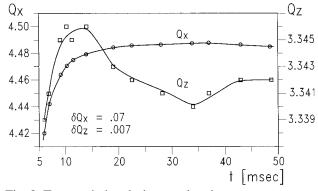

Fig. 3: Tune variation during acceleration.

Figure 3 shows the tune during the acceleration cycle with a total variation of $\delta Q_x = 0.07$ and $\delta Q_z = 0.007$ better than specified. The largest variations occur within

the first 10 msec after injection i.e. at low field. These variations may be atributed i) to variations of the effective length of the quadrupoles relative to the dipoles generated by permeability changes at low excitation, and ii) to time-dependent fields induced by eddy currents in the vacuum chambers of the dipoles [6] and quadrupoles [7]. At higher energy the variations are negligible as with a maximum pole tip field of 1 T for the quads and the dipoles there is practically no saturation.

The chromaticities measured with the same technique show significant deviations from the natural chromaticities $\xi_{x/z} = - 4.7/-3.9$ of the design optics (see Fig. 4). In contrast to the tune and the orbit, the chromaticity varies over the whole acceleration cycle, which indicates that eddy current effects are not dominant. We have fitted an integral sextupole m·l in the dipole to each $\xi_{x/z}$-measurement with the result of a nearly linear decrease of the sextupole during acceleration. Qualitatively this is what we expect from the dipole with its strongly shimmed pole contour to improve the good field range at full excitation. The linear variation of m·l fits the $\xi_{x/z}$-data nicely at higher fields and gives the natural chromaticity for m·l =0 with reasonable accuracy. The deviations at lower energies may be attributed to an eddy current driven sextupole in the dipole chamber.
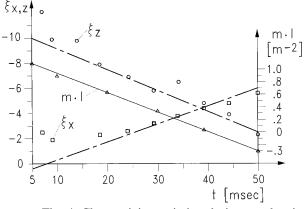

Fig. 4: Chromaticity variation during acceleration and integral sextupole strength m·l of the dipole obtained from a fit.

3.3 Orbit Variations

The BPM system allows to measure orbits in 256 time bins of 200 μs width, providing a versatile tool for the analysis of orbit variations during acceleration. Details of the electronics and the software are described in [8]. During acceleration there is no significant variation of the vertical orbit to be seen and the deviations $\Delta y = \pm 1.5$ mm are comparable with the systematic positioning errors of the BPM's as in DC-operation. Horizontally, however, the orbit errors at injection are about a factor of 2.5 larger than in DC-operation. They decrease rather quickly with increasing energy down to $\Delta x = \pm 3$ mm at about 400 MeV and stay then constant up to the max. energy (see

Fig. 5). The energy independent part corresponds roughly with the max. deviations observed in DC-operation as (ch.2.2). The energy dependent part must be attributed to different dynamic behaviour of the dipoles: permeability variations at low excitation, fields generated by eddy currents in the vacuum chamber [6], and capacitive leakage currents to earth from the cables connecting the dipoles.
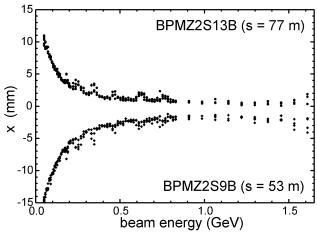

Fig. 5: Energy dependence of the max. horizontal orbit deviation.

4 SUMMARY

The BESSY II booster synchrotron has shown very stable operation during the first 12 months, which made commissioning rather simple and straight forward. This can be attributed mainly to the IGBT-controlled AC power supplies and to the control electronics of the whole White circuit system.

5 ACKNOWLEDGEMENT

REFERENCES

[1] E. Weihreter, Techn. Report BESSY II, TB No.174 (1993)
[2] M. Abo-Bakr et al., Proc. Europ. Part. Acc. Conf., 1996, p.527
[3] T. Knuth, D. Krämer, E. Weihreter, I. Chertok, S. Michailov, B. Sukhina, IEEE Part. Acc. Conf. 1996, p. 1316
[4] K. Bürkmann et al., this conference
[5] D. Schirmer, M.v.Hartrott, S. Khan, D. Krämer, E. Weihreter, IEEE Part. Acc. Conf. 1996, p. 1879
[6] H. Hemmie, J. Rossbach, DESY M84-05, 1984
[7] B. N. Zhukov, V.N. Lebedev, Pribory i Tekhnika, Eksperimenta, No 5, p. 26 (1973)
[8] R. Bakker et al., this conference